

Photonic Implementation of the Quantum Morra Game

Andrés Ulibarrena,¹ Alejandro Sopena,² Russell Brooks,¹ Daniel Centeno,^{2,3,4} Joseph Ho,¹ Germán Sierra,² and Alessandro Fedrizzi¹

¹*Institute of Photonics and Quantum Sciences, School of Engineering and Physical Sciences, Heriot-Watt University, Edinburgh EH14 4AS, United Kingdom*

²*Instituto de Física Teórica, UAM-CSIC, Universidad Autónoma de Madrid, Cantoblanco, 28049 Madrid, Spain*

³*Perimeter Institute for Theoretical Physics, Waterloo, Ontario, Canada, N2L 2Y5*

⁴*Department of Physics and Astronomy, University of Waterloo, Waterloo, Ontario, Canada, N2L 3G1*

The Morra game, an age-old non-cooperative game, traditionally played on one's hand, has proved to be a rich setting to study game-theoretic strategies, both classically and within the quantum realm. In this paper, we study a faithful translation of a two-player quantum Morra game, which builds on previous work by including the classical game as a special case. We propose a natural deformation of the game in the quantum regime in which Alice has a winning advantage, breaking the balance of the classical game. A Nash equilibrium can be found in some cases by employing a pure strategy, which is impossible in the classical game where a mixed strategy is always required. We prepared our states using photonic qubits on a linear optics setup, with an average deviation $\leq 2\%$ with respect to the measured outcome probabilities. Finally, we discuss potential applications of the quantum Morra game to the study of quantum information and communication.

I. INTRODUCTION

Modern game theory, initially developed by J. Nash and J. Neumann [1, 2] for analysing economic strategies among rational players in a mathematically consistent model, has found widespread applications in various fields, including biology [3], politics [4], choice-theory [5] and computer science [6]. However, the emergence of quantum information in the 80's and 90's enabled researchers to study game theoretic models in the quantum regime and it has turned out that superposition and entanglement allow new winning strategies that previously did not exist [7, 8]. Quantum games (QG) have already been used to design quantum cryptographic protocols with enhanced security [9, 10] and optimise networks for frequency allocation [11]. Moreover, studying QG's has revealed new insights on non-cooperative games such as prisoners dilemma where a new equilibrium strategy was found and improved the payoff to all players [12, 13]. Quantum games can now be implemented on plethora of systems, such as small-scale quantum processors [14], ion traps [15] or nitrogen vacancies in diamonds [16] however the most common platform has been photonics [17–20]. This has the benefit that the games can be played between remote players, and that they can then be used as primitives for higher level distributed quantum communication tasks [21].

Here we consider one of the oldest known games that is still studied today, the Morra game [22, 23]. Morra is a non-cooperative game in which players hide a maximum number of coins (*or fingers*), and each player attempts to guess the total number. Players are ordered a priori, and the rule is that a player cannot repeat the guess of the previous ones. This rule apparently gives the first player an advantage over the rest, but unexpectedly everyone has an equal chance of winning. The Morra is a closely related game to the Spanish Chinos game, which has been studied extensively [24, 25]. The Morra's game

has applications in modelling financial markets, and information transmission [24].

Quantum versions of Morra's game have been proposed in the past [26, 27], with the aim of studying the equilibrium strategies between the two players. The basic idea is to replace the act of drawing a coin by that of applying an operator on a quantum state shared by all players, say a boson, or a hard-core boson (fermions), a qubit, or two qubits. These operations create a state in which one measures an observable that is the classical analogue of the total number of coins. In some situations quantum effects may lead to the breaking of the classical balance of the players.

Here we show a novel implementation of the quantum Morra game (QMG) using qutrits that, unlike the previous proposals [26, 27], can reproduce the classical game faithfully. This version of the game allows us to deform the underlying rules, which we shall define later, thereby generating new effects. This implementation makes use of a three level system as shared resource for players to act on, similar to the Aharonov three quantum boxes game [16]. We implement this game employing entangled photonic qubits and obtained good agreement between the theory and the experimental results.

A. Classical Morra Game

We shall consider the simplest version of the Morra game that involves two players, Alice and Bob, who can draw each from 0 to 1 coins and guess the total number of coins with the restriction that Bob cannot repeat the result predicted by Alice. This game can be generalised to more players and coins [26]. We distinguish between pure strategies, which involve players selecting a specific number of coins, and mixed strategies, where players randomize their coin choices based on probabilities assigned to each possible number of coins. A non-cooperative game

which allows mixed strategies is guaranteed to have at least one Nash equilibrium [28], a situation where neither player can improve their payoff by unilaterally changing their strategy, as long as their opponent does not change their strategy. We refer to a strategy as optimal when it leads to a Nash equilibrium [2].

The optimal strategy for Alice is to choose at random $c_A = 0, 1$ coins and to guess always $g_A = 1$, so as not to reveal information to Bob [26]. This is based on the fact that with four possible outcomes, the most probable value of the sum is 1. Bob's optimal strategy is to choose $c_B = 0, 1$ coins at random and make his guess g_B in a rational way [29].

A rational player seeks to maximise their expected payoff or benefit [30]. For example, users competing for bandwidth in a radio network [31], or prisoners minimising their jail sentence [12]. In the context of the Morra game, if Bob chooses $c_B = 0$, then by reason he must exclude the option $g_B = 2$, and if he chooses $c_B = 1$, then he must exclude $g_B = 0$. Playing the optimal strategy, each player wins on average half of the time, resulting in a symmetric game with equal winning probabilities.

This strategy is also Pareto optimal [32], since no player can improve their own payoff without reducing their opponents payoff. In game theory, this scenario is called a zero-sum game [1]. This result is also valid for two players and a general number of coins [26].

II. QUANTUM MORRA GAME

In our version of the QMG, first we will associate the total number of coins, namely 0, 1, 2, to three orthogonal states $|\tilde{0}\rangle, |\tilde{1}\rangle, |\tilde{2}\rangle$ that form the basis of a qutrit. To produce these states, the players have two unitary operators, \mathcal{O}_0 and \mathcal{O}_1 , that correspond to the number of coins they have in their hands at the start of each roll. The joint state created by Alice and Bob is given by

$$|\psi_{a,b}\rangle = \mathcal{O}_a^A \mathcal{O}_b^B |\phi\rangle, \quad a, b = 0, 1, \quad (1)$$

where $|\phi\rangle$ is an initial state and note $|\psi_{0,1}\rangle$ and $|\psi_{1,0}\rangle$ are identical states (a relative phase between them is unobservable). Using this equation the basis states are obtained as $|\tilde{0}\rangle = |\psi_{0,0}\rangle$, $|\tilde{1}\rangle = |\psi_{0,1}\rangle = |\psi_{1,0}\rangle$ and $|\tilde{2}\rangle = |\psi_{1,1}\rangle$. Choosing \mathcal{O}_0 as the identity operator we find that $|\phi\rangle = |\tilde{0}\rangle$ and

$$|\tilde{1}\rangle = \mathcal{O}_1 |\tilde{0}\rangle, \quad |\tilde{2}\rangle = \mathcal{O}_1^2 |\tilde{0}\rangle. \quad (2)$$

The operator \mathcal{O}_1 has to be unitary. A solution compatible with (2) is $\mathcal{O}_1 = X$, where X is the Pauli matrix for qutrits,

$$X = \begin{pmatrix} 0 & 0 & 1 \\ 1 & 0 & 0 \\ 0 & 1 & 0 \end{pmatrix}, \quad (3)$$

that satisfies $X^3 = \mathbb{I}$. In the quantum game, the operator X^3 never arises because the maximum number of X operators is 2. However, we shall consider that having three coins in the box is the same as having none.

The outcome of a round of the game is determined by measuring the observable

$$\hat{N} = \sum_{n=0}^2 n |\tilde{n}\rangle \langle \tilde{n}|. \quad (4)$$

The state after such measurement will be $|\tilde{0}\rangle, |\tilde{1}\rangle$, or $|\tilde{2}\rangle$, thereby revealing the number of coins. The winner of the round is the player whose guess matches the number of coins. Our game can be generalised to n -players, which we show in Appendix E. The scalability of potential moves improves within this encoding scheme compared to previous implementations [26, 27] due to the binary choice of the coin operator. The original game employed four operators [26] and the single qubit game uses three operators [27]. Consequently, our game scales as 2^N , where N is the number of players, compared to the previous 4^N and 3^N for the respective games.

A. Quantum Deformation

In this section we will precisely define what a deformation is in the context of our game. We are specifically referring to the players encoding operator (3) that controls the unitary evolution of the shared state, and the underline probability distribution of the game. To go beyond the classical setting we use a parameter θ to smoothly deform the operator away from (3). The physical meaning of this deformation is that the players are able to toss a certain superposition of the number of coins instead of just the classical options.

We have translated the classical Morra game into a quantum game by means of a one-to-one correspondence between classical and quantum objects. The quantum realm allows us to define the superposition of coin states, in analogy to the superposition of cat states. For this we use the quantum Fourier transform

$$\mathcal{F}|\tilde{j}\rangle = \frac{1}{\sqrt{3}} \sum_{k=0}^2 \omega^{jk} |\tilde{k}\rangle, \quad \omega = e^{2i\pi/3}. \quad (5)$$

Measuring the number of coins in each of the states (5) yields the values 0, 1 or 2 with equal probability $1/3$. Moreover, applying the operator X to (5), that is *adding* a quantum coin, just multiply these states by a global phase, $X|\tilde{j}\rangle = \omega^{-j} |\tilde{j}\rangle$.

Along with the Pauli matrix X for qutrits (3), there is a matrix Z defined as $Z = \text{diag}(1, \omega, \omega^2)$ that satisfies $ZX = \omega XZ$ and is related to X by the Fourier transform

$$X = \mathcal{F}^\dagger Z \mathcal{F}, \quad (6)$$

where $\mathcal{F}_{j,j'} = \frac{1}{\sqrt{3}}\omega^{jj'}$ ($j, j' = 0, 1, 2$). This connection will allow us to deform the quantum game from the phase space.

The two players game can be deformed by replacing Z in (6) by $Z_\theta = \text{diag}(1, e^{i\theta}, e^{2i\theta})$ yielding a modified X operator,

$$X_\theta = \mathcal{F}^\dagger Z_\theta \mathcal{F} = \begin{pmatrix} x_0(\theta) & x_2(\theta) & x_1(\theta) \\ x_1(\theta) & x_0(\theta) & x_2(\theta) \\ x_2(\theta) & x_1(\theta) & x_0(\theta) \end{pmatrix}, \quad (7)$$

where

$$x_j(\theta) = \frac{1}{3}(1 + \omega^{2j}e^{i\theta} + \omega^j e^{2i\theta}). \quad (8)$$

The states created by the action of X_θ are

$$|1_\theta\rangle = X_\theta|\tilde{0}\rangle = x_0(\theta)|\tilde{0}\rangle + x_1(\theta)|\tilde{1}\rangle + x_2(\theta)|\tilde{2}\rangle, \quad (9)$$

$$|2_\theta\rangle = X_\theta^2|\tilde{0}\rangle = x_0(2\theta)|\tilde{0}\rangle + x_1(2\theta)|\tilde{1}\rangle + x_2(2\theta)|\tilde{2}\rangle, \quad (10)$$

where we used that $X_\theta^2 = X_{2\theta}$. These states are normalised but are not orthogonal except for $\theta = 2\pi/3$ and $4\pi/3$. We have found a general two-qubit quantum circuit for the deformation unitary (7) using eight local unitaries and three CNOT gates [33, 34], as outlined in the Appendix D. Regarding the physical interpretation of the deformation, (9) tells us that, now, there exists the possibility of one player tossing two coins with a certain probability although in the classical version they only have one coin in their hands.

We recall that the probabilities are given by,

$$p_{a,b}(n) = |\langle n|\psi_{a,b}\rangle|^2 \quad (11)$$

where $|n\rangle$ are the states $|\tilde{0}\rangle, |\tilde{1}\rangle, |\tilde{2}\rangle$ and $|\psi_{a,b}\rangle$ are the common states generated by Alice and Bob using the operators X_θ and X_θ^2 . In particular the average probabilities of Alice are given by $P_a(n) = \frac{1}{2}\sum_b p_{a,b}(n)$, which becomes

$$P_a(n) = \frac{1}{2}(|x_n(a\theta)|^2 + |x_n((a+1)\theta)|^2) \quad (12)$$

III. EXPERIMENTAL IMPLEMENTATION

We experimentally realise the QMG with a linear optics circuit, using polarisation encoded photons to prepare a two-qubit state. We can write the qutrit state $|\tilde{a}\rangle$ as a two-photon state $|i_A i_B\rangle$ where $(i_A, i_B = H, V)$ are the horizontal and vertical polarisation states of each photon and the indices indicate a different photon mode. The qutrit to qubit transformation can be found in the

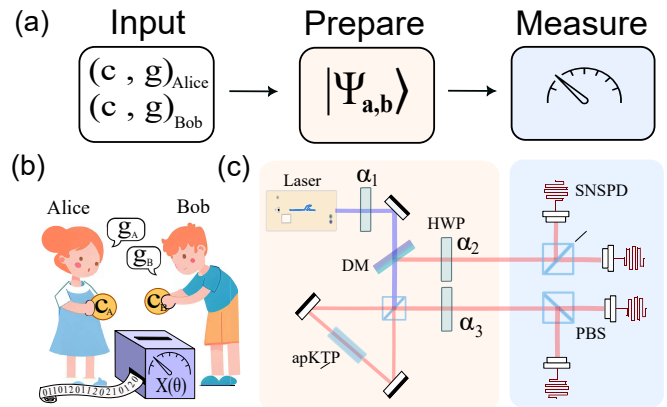


FIG. 1. The QMG experimental implementation. (a) Alice and Bob's strategies are input into a device which prepares the joint state $|\psi_{a,b}\rangle$ and subsequently measures it. (b) Alice and Bob play the QMG by secretly depositing coins c_A and c_B into the device which has some pre-determined parameter θ . Alice makes the first guess g_A , followed by Bob g_B . The device deforms the classical coins into quantum coins using the Unitary $X(\theta)$, performs a measurement and outputs the sum of the coins. (c) The linear optics circuit for state preparation begins with a photon pair source, constructed with a apKTP crystal housed in a Sagnac configuration [35, 36] pumped with a ti:sapphire laser centered at 775 nm and prepared in H with a linear polariser (POL), producing degenerate photon pairs at 1550 nm, which are separated from the pump with a dichroic mirror (DM). The states $|\psi_{a,b}\rangle$ are encoded using the three half-wave plates (HWP) $\alpha_1, \alpha_2, \alpha_3$, outlined in the Appendix C. The measurement station consists of two polarising beam splitters (PBS) that project the two photons into the Z-basis, then coupled to superconducting nanowire single photon detectors (SNSPD), and 2-fold coincidences are identified using a time-tagging logic box.

Appendix B, where we arrive at the same encoding states,

$$|\tilde{0}\rangle = |HH\rangle, \quad (13)$$

$$|\tilde{1}\rangle = \frac{1}{\sqrt{2}}(|HV\rangle + |VH\rangle), \quad (14)$$

$$|\tilde{2}\rangle = |VV\rangle, \quad (15)$$

Figure 1 shows our experiment outlined in three stages; Alice and Bob input their coin choice to the device, the device prepares the shared state, and finally measures the outcome. We prepare our states (9) and (10) using the parameterised half-wave plate configuration $(\alpha_1, \alpha_2, \alpha_3)$. We used solutions that match the desired outcome probability of the shared state and preserve the entanglement entropy. We reframe the problem as an optimization problem and determine the solution with the L -BFGS-B algorithm [37] implemented in SciPy [38], as outlined in the Appendix C. These states require high fidelity and purity to recreate the game faithfully, so we take advantage of a bright photon-pair source using an aperiodically-poled potassium titanyl phosphate

(apKTP) crystal, which creates spectrally pure entangled photon pairs via spontaneous parametric down-conversion (SPDC) [39, 40].

A. Results

Approximately 150 000 rounds are played for 34 evenly spaced values of θ in the interval $[0, 2\pi]$. The data collection methods are discussed in Appendix A. The normalised probabilities for states $|1_\theta\rangle$ and $|2_\theta\rangle$ can be found in Appendix C. To analyse how these new outcome probabilities affect the players strategies we have averaged Bob's two plays over each of Alice's choices using (12). The results have been plotted in Figure 2a when Alice plays zero coins, and Figure 2b when Alice plays one coin. The experimental values closely align with the theoretical expectation, deviating by a maximum of 2% and confirms a successful implementation of the QMG. We have measured a fidelity, compared to the ideal states $|\tilde{0}\rangle$, $|\tilde{1}\rangle$ and $|\tilde{2}\rangle$, of 97%. The main causes for the uncertainties in our experimental data are due to factors such as imbalances on the PDC photon generation loop, losses and depolarisation on the single-mode fibres and imperfections in the retardance of the half waveplates.

In Table I we summarise the most notable points in the Figure 2, where $P_i(G)$ is Alice's probability of winning by guessing G when playing i coins.

At θ values close to $2\pi/3$, the classical regime is recovered, matching the values predicted by the theory in Figure 2. Similarly, at $4\pi/3$, the classical probabilities are reproduced, but the guesses for coins 1 and 2 are flipped. This creates a classically impossible situation since Alice plays no coins and can expect a 50% probability of winning by guessing 2 coins.

Notably, for θ equalling 0 and 2π , the game undergoes a complete deformation, resulting in all coin states overlapping into the 0 coin outcome, as we can see in Table I. In this case, Alice will always win if she guesses 0 coins, regardless of the number of coins in play.

When $\theta = \pi$, the probable outcome for each coin is identical regardless of the coin Alice picks. Even so, Alice still has an advantage over Bob as guessing $|\tilde{0}\rangle$ yields a winning result higher than 0.5.

| θ | 0 | $2\pi/3$ | π | $4\pi/3$ |
|----------|----------------------|----------------------|-------|----------------------|
| $P_0(0)$ | 0.99 | 0.50 | 0.57 | 0.51 |
| $P_0(1)$ | $1.19 \cdot 10^{-3}$ | 0.49 | 0.30 | $1.43 \cdot 10^{-3}$ |
| $P_0(2)$ | $7.63 \cdot 10^{-3}$ | $2.46 \cdot 10^{-3}$ | 0.13 | 0.49 |
| $P_1(0)$ | 0.98 | $7.86 \cdot 10^{-3}$ | 0.57 | $1.26 \cdot 10^{-2}$ |
| $P_1(1)$ | $2.46 \cdot 10^{-3}$ | 0.50 | 0.30 | 0.49 |
| $P_1(2)$ | $1.67 \cdot 10^{-4}$ | 0.49 | 0.13 | 0.49 |

TABLE I. Alice's probability of winning (P_i) for different θ values, depending on the amount of coins in play (i).

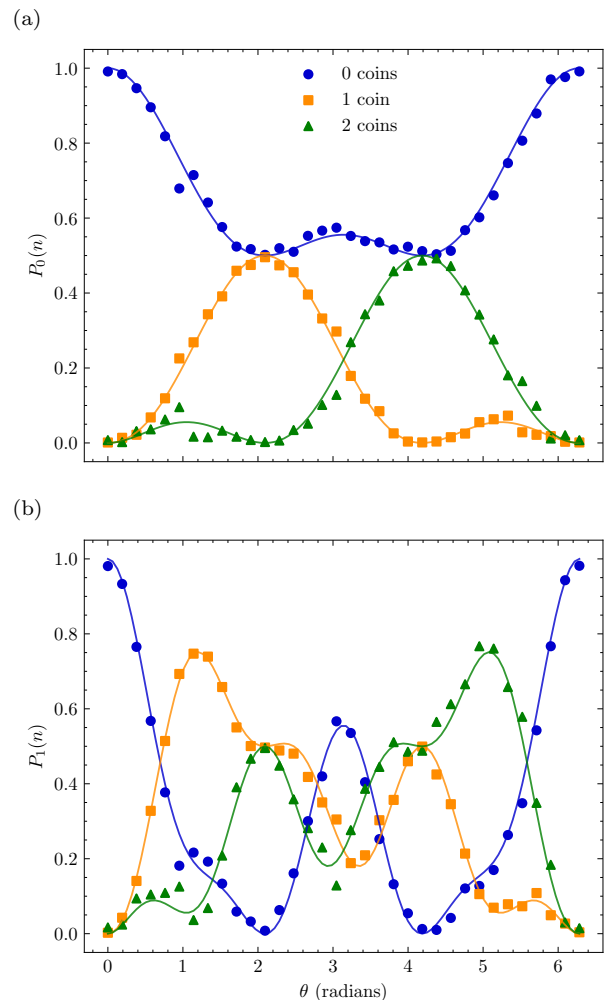


FIG. 2. Alice's probability of winning versus θ , when playing 0 and 1 coin. The probabilistic outcome of obtaining (0,1,2) coins when Alice plays no coins (II) (a) and when she plays one coin (b) have been plotted on top of the theoretical curves. Errors bars have calculated assuming Poisson statistics, but found to be $\mathcal{O}(10^{-4})$, therefore neglected.

IV. STRATEGIES

The deformation θ opens up the possibility for new strategies in which Alice's winning probability is higher than 50%. We focus on analysing the best strategies for each player when they play randomly, as well as characterising the optimal strategy as a function of the deformation. Each player's strategy is defined by the probability of playing zero or one coin, as well as their guesses for each situation. Since Alice plays first, we consider strategies in which her guess is independent of the number of coins she plays, in order to not reveal information, similarly to the classical case. The winning probability of Alice given a strategy where she plays a coins with probability \tilde{P}_a^A and guesses n coins, while Bob plays b coins

with probability \tilde{P}_b^B is

$$P_{win}^A = \sum_{a,b} \tilde{P}_a^A \tilde{P}_b^B p_{a,b}(n), \quad (16)$$

where $p_{a,b}$ is given in (11). On the contrary, Bob can change his guess n_b based on the number of coins he plays, but it must be different from Alice's guess. The winning probability of Bob is

$$P_{win}^B = \sum_a \tilde{P}_a^A (\tilde{P}_0^B p_{a,0}(n_0) + \tilde{P}_1^B p_{a,1}(n_1)). \quad (17)$$

We say that a player's strategy is stable when his probability of winning is higher than that of the other players even if they change their strategies.

In the classical game, it is possible to achieve a Nash equilibrium with a mixed strategy where each player wins half the time by choosing 0 or 1 coins at random. However, the deformation θ allows Alice to have an advantage over Bob when both playing randomly because she can make guesses that increase her winning probability or the draw probability as shown in Figure 3a. In general, these strategies are not stable, and both Alice and Bob can improve them, provided they know each other's strategies. Although Alice's winning probability is higher than Bob's, she can further increase it, as shown in Figure 3b. Bob can try to improve his strategy as well, but in some cases, he is unable to turn the situation around, and Alice's winning probability remains higher as shown in Figure 3c. In these cases, Alice's strategy is stable, although not optimal.

Figure 3 allows us to verify if there are values of θ that allow an optimal strategy when playing randomly apart from the classical case. This is possible for $\theta = 4\pi/3$ since it is equivalent to the classical case under the exchange of states $|1_\theta\rangle$ and $|2_\theta\rangle$. Remarkably, for $\theta = \pi$, it is also possible to achieve equilibrium by playing randomly, although Alice's winning probability is higher than Bob's. In this case, Alice must guess zero coins and Bob one or two. For other values of theta, Alice and Bob's improved strategies are pure. For instance, in the optimal strategy for $\theta = \pi/3$, Alice consistently plays 0 coins and guesses 0, while Bob plays 1 coin and guesses 1. In this scenario, Alice's winning probability is 0.46, Bob's winning probability is 0.44, and the probability of a draw is 0.1. This case highlights the counterintuitive nature of the deformed game, as in classical terms, this strategy would allow Bob to win every time.

A. Optimal strategies

We have calculated the winning probabilities for each player using the experimental data for the overlaps, demonstrating a strong agreement with the theory (see Figs. 4 and 3). One may wonder how the optimal strategy of each player changes depending on the θ deforma-

tion. To find these strategies, we utilize an exhaustive search approach. Initially, we define Alice's strategy and identify the strategy for Bob to maximize his winning probability. Then, we check whether the best strategy for Alice, considering Bob's strategy, aligns with our initial choice. If this is the case, these strategies establish a Nash equilibrium; otherwise, we iterate the process by changing Alice's strategy. It is important to note that these strategies rely on information from both players. Therefore, it would not be possible for either of them to discover these strategies beforehand due to the lack of complete information. The winning probabilities for each player when following the optimal and stable strategy as a function of θ are shown in Figure 4. These strategies are mixed for $\theta \in [4\pi/9, 14\pi/9]$, while for the remaining values, they are pure. The transition between mixed and pure strategies occurs at non-trivial θ values, these are determined by the construction of the operator $X(\theta)$. Multiple applications of $X(\theta)$ will change the phase relation between the states, which can be seen in the exponent of 8, therefore this transition point is expected to be different with more players.

V. DISCUSSION AND CONCLUSION

In contrast to the classical game, the deformation θ gives Alice an advantage because she wins more often than Bob, and Bob cannot do anything to change it. Another significant aspect that sets it apart from the classical case is the possibility of both players losing. When playing optimally, the classical game has been shown to be a zero-sum game. This is not true for the quantum game and is more likely to occur at $\theta = \pi$ where there is a 20% chance that nobody wins. Moreover, the Nash equilibrium outside the classical case is no longer Pareto-optimal except at $\theta = 0, 4\pi/3$ and 2π .

The search for an optimum strategy using shared resources is closely aligned with other competitive games, such the spectrum scarcity problem [11]. Our analysis has shown that sometimes pure or mixed strategies are available, but may come with different resource overheads. However, we did not consider these resource costs in this paper and leave it as an open problem for future work.

A natural extension of the current implementation is to a three player game, since the four possible outcomes can be encoded on just two photons. In fact, the number of qubits scales as $\lceil \log_2(M+1) \rceil$ (see Appendix E) where M represents the total number of coins, allowing for the efficient construction of a network of players. Moreover, the selection of basis states in this implementation remains arbitrary; we could have opted for three distinct Bell pairs to encode $|\tilde{0}\rangle$, $|\tilde{1}\rangle$ and $|\tilde{2}\rangle$. Using entangled states with minor modifications to the game, could open the possibility of non-local strategies enabled by quantum steering [41, 42]. This raises the question whether quantum games can be exploited within the network con-

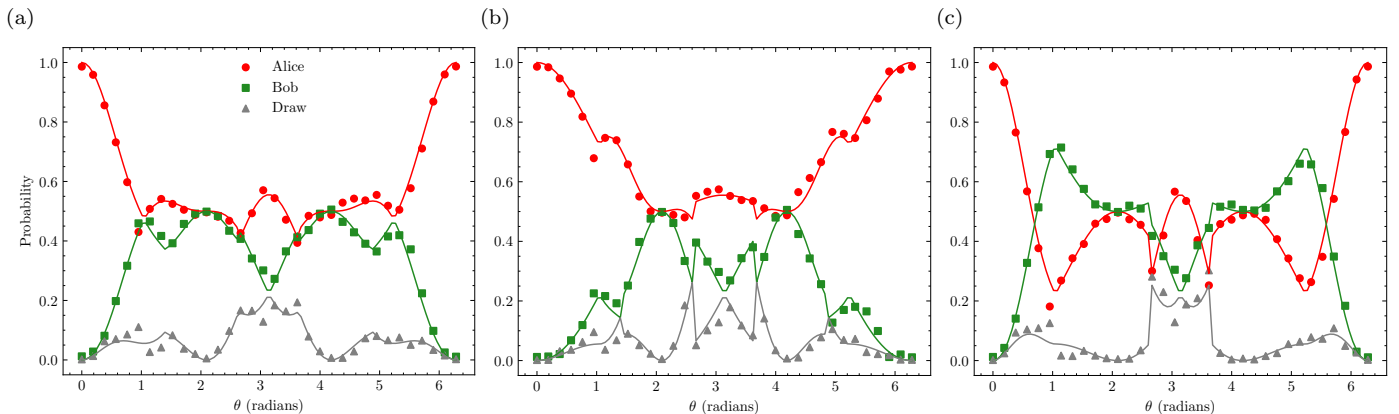


FIG. 3. (a) The winning probabilities of Alice (red) and Bob (green), as well as the probability of a draw (gray), when both players choose 0 or 1 coin at random but make their best guess. (b) Alice plays her best strategy knowing that Bob plays randomly. (c) Bob plays his best strategy knowing that Alice plays randomly. The experimental results have been plotted on top of the theoretical values.

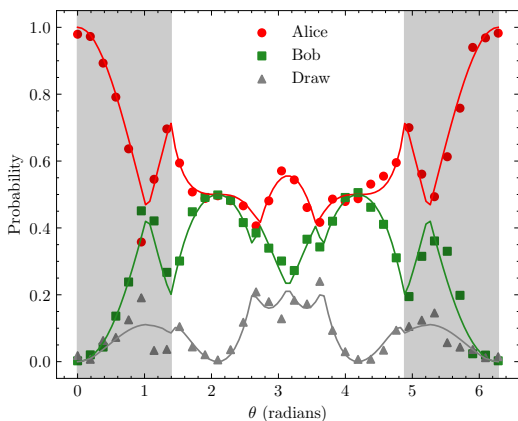


FIG. 4. Optimal strategies for Alice and Bob. The winning probabilities for Alice (red) and Bob (green) are shown when each of them plays with their best strategies. The probability of a draw, where neither of them wins, is indicated in gray. The shaded area shows the values of θ for which the strategies are pure. The experimental results have been plotted on top of the theoretical values.

text [21], that gain an advantage from multi-partite resources [36, 43].

In summary, we have outlined a new construction of the two-player quantum Morra game, providing Alice with a winning advantage over Bob that surpasses the classical game. The deformation operator and theoretical states have been realized within a linear optics setup, achieving high fidelity and low standard deviation with respect to the measurement outcomes, which is less than 2%.

This formulation of the quantum Morra game has bridged the classical and quantum domains by incorporating the classical game as a particular instance within the extended quantum game. In analysing the strategies,

we have identified a new Nash equilibrium that diverges from the classical game. This has enhanced our understanding of strategies in quantum game theory and provided insight into the realization of new quantum games. Surprisingly, it remains unknown whether the equivalent of a Kakutani fixed-point theorem exists in a complex space, such a discovery would guarantee a Nash equilibrium for all quantum games [44]. Therefore, further theoretical development in quantum game theory is needed to support the implementation of more complex quantum games.

Finally, by extending the principles and techniques applied in this work to other quantum games, we can potentially evaluate the robustness and efficiency of quantum communication networks and deepen our understanding of quantum game theory.

ACKNOWLEDGMENTS

This work was supported by the UK Engineering and Physical Sciences Research Council (Grant Nos. EP/T001011/1.) A.S. is supported by the Spanish Ministry of Science and Innovation under the grant SEV-2016-0597-19-4. G.S. acknowledges the support of the Spanish Research Agency (Agencia Estatal de Investigación) through the grants “IFT Centro de Excelencia Severo Ochoa CEX2020-001007-S” and PID2021-127726NB-I00, funded by MCIN/AEI/10.13039/501100011033 and by ERDF, as well as from the CSIC Research Platform on Quantum Technologies PTI-001. DC is supported by Perimeter Institute for Theoretical Physics. Research at Perimeter Institute is supported in part by the Government of Canada through the Department of Innovation, Science and Economic Development and by the Province of Ontario through the Ministry of Colleges and Universities.

APPENDICES

The Appendices are organised as follows: Appendix A provides additional details on the experimental setup. Appendix B provides a detailed description of the qutrit-to-qubit mapping required for the experimental implementation of the game. The computation of waveplates parameters and experimental overlaps is covered in Appendix C. Additionally, the unitary transformation is decomposed into one-qubit gates and CNOT gates in Appendix D. Appendix E generalises the deformed game to N players and M coins. Finally, Appendix F introduces the novel concept of Quantum Deposit, drawing inspiration from the quantum Morra game.

Appendix A: Methods

We prepare our states using a photon source housed in a Sagnac interferometer to control the PDC process. Figure 5 shows a Ti-Sapph laser pumping an aperiodically-polled potassium titanyl phosphate, crystal with 774.8nm light, creating spectrally degenerate photons at 1549.6nm. A lens focuses the beam onto the crystal for optimum PDC events and a Glan-Taylor prism ensures only linearly polarised light enters the Sagnac while a Dichroic Mirror reflects only down converted photons towards the coupler.

The first Half Wave Plate (HWP I) engineered for 775nm and the the Dual-wavelength Polarisation Beam Splitter (DPBS) control the pump direction into transmitted and reflected spatial modes around the Sagnac; Horizontal for clockwise direction and Vertical for Anti-clockwise (AC). A dual-wavelength half-waveplate inside the Sagnac loop rotates V-pol light (In the reflected port) into H-pol to facilitate PDC in the counter-propagating direction. When pumping with D-pol light, the signal and idler photons are indistinguishable and create a maximally entangled state (A1).

$$|\Psi^+\rangle = \frac{1}{\sqrt{2}}|h_s v_i\rangle + e^{i\phi}|v_s h_i\rangle \quad (\text{A1})$$

We optimise the phase component from to the fibers and mirrors acting on the two qubits using Polarisation Fiber Controllers (PFC) and recover the Ψ^+ . Down converted signal and idler photons exit the DPBS and are rotated by two 1550nm HWP's (II,III), parameterised by the numerical solution to the Unitary (B11) and coupled into a Single Mode Fiber.

The single photons detected on SNSPs are counted using a logic box to identify coincidence events in the four detector patterns shown in Fig. 6. Approximately 150 000 rounds where conducted for 34 evenly spaced values in the interval $[0, 2]$.

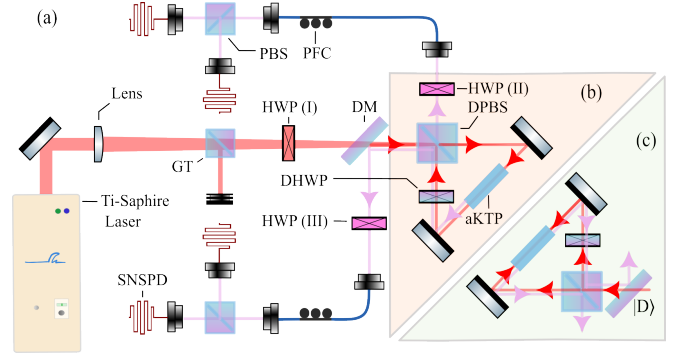


FIG. 5. (a) The linear optics circuit, (b) the encoding scheme for $|HH\rangle$ configuration when pumping in Horizontal polarisation and waveplates $\{I,II,III\}$ (c) Pumping with D polarised light. Components: Glan-Taylor (GT), Half Wave Plate (HWP), Dual-wavelength Polarisation Beam Splitter (DPBS), Dichroic Mirror (DM), dual-wavelength HWP (DHWP), Single Mode Fiber (SFM), Polarising Beam Splitter (PBS), Superconducting Nano-wire Single Photon Detectors (SNSPD), aperiodically-polled potassium titanyl phosphate (aKTP).

Appendix B: From qutrits to qubits

Let us denote by $|i_A i_B\rangle$, ($i_A, i_B = 0, 1$) a basis of two qubits states. The qutrit states will be defined as

$$|\tilde{0}\rangle = |00\rangle, \quad (\text{B1})$$

$$|\tilde{1}\rangle = \frac{1}{\sqrt{2}}(|01\rangle + |10\rangle), \quad (\text{B2})$$

$$|\tilde{2}\rangle = |11\rangle. \quad (\text{B3})$$

Equation (3) of the main text expresses X in the qutrit basis $|I\rangle$ ($I = \tilde{0}, \tilde{1}, \tilde{2}$). To implement the operation X on two qubit states we have to extend the basis $|I\rangle$ to a fourth vector

$$|\tilde{3}\rangle = \frac{1}{\sqrt{2}}(|01\rangle - |10\rangle) \quad (\text{B4})$$

and promote $X \rightarrow X_4$ that acts according to

$$|\tilde{1}\rangle = X_4|\tilde{0}\rangle, \quad |\tilde{2}\rangle = X_4^2|\tilde{0}\rangle, \quad (\text{B5})$$

and trivially on (B4)

$$X_4|\tilde{3}\rangle = |\tilde{3}\rangle. \quad (\text{B6})$$

The matrix X_4 reads in the basis $|I\rangle$ ($I = \tilde{0}, \tilde{1}, \tilde{2}, \tilde{3}$)

$$X_4 = \begin{pmatrix} 0 & 0 & 1 & 0 \\ 1 & 0 & 0 & 0 \\ 0 & 1 & 0 & 0 \\ 0 & 0 & 0 & 1 \end{pmatrix}. \quad (\text{B7})$$

To find the action of X_4 on the two qubit states we use the unitary transformation V that expresses the basis $|I\rangle$

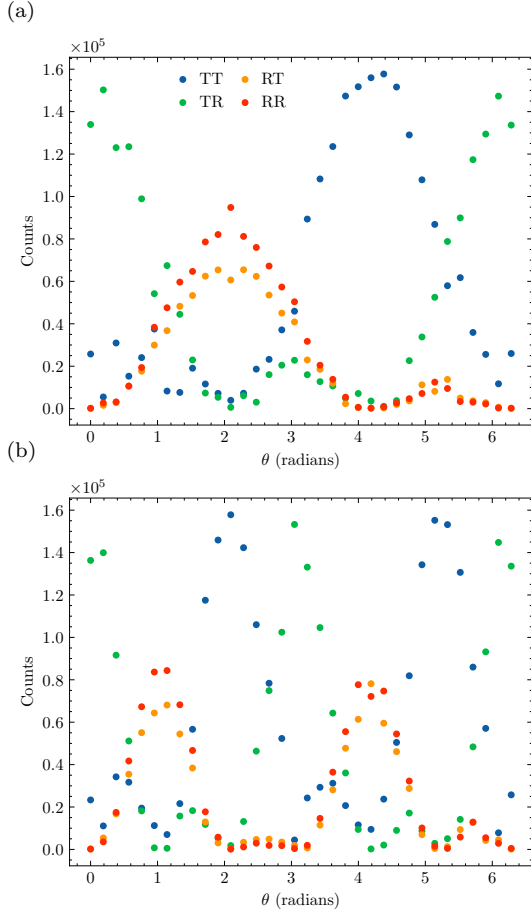


FIG. 6. The coincidence counts on each of the 4 pairs of detectors coupled to the Transmitted (T) and Reflected (R) ports of the PBS to reproduce the overlaps for the states $|1_\theta\rangle$ (a) and $|2_\theta\rangle$ (b). Error bars have been calculated with Poissonian statistics, but omitted due to size.

in terms of the basis $|i_A i_B\rangle$

$$|I\rangle = \sum_{i_A i_B} V_{i_A i_B, I} |i_A i_B\rangle, \quad I = \tilde{0}, \tilde{1}, \tilde{2}, \tilde{3} \quad (\text{B8})$$

where

$$V = \begin{pmatrix} 1 & 0 & 0 & 0 \\ 0 & \frac{1}{\sqrt{2}} & 0 & \frac{1}{\sqrt{2}} \\ 0 & \frac{1}{\sqrt{2}} & 0 & -\frac{1}{\sqrt{2}} \\ 0 & 0 & 1 & 0 \end{pmatrix}. \quad (\text{B9})$$

The rows are labelled by 00,01,10,11 and the columns by $\tilde{0}, \tilde{1}, \tilde{2}, \tilde{3}$. The matrix expressing the action of X_4 in the two qubit basis is given by

$$X_{2 \times 2} = V X_4 V^\dagger = \begin{pmatrix} 0 & 0 & 0 & 1 \\ \frac{1}{\sqrt{2}} & \frac{1}{2} & -\frac{1}{2} & 0 \\ \frac{1}{\sqrt{2}} & -\frac{1}{2} & \frac{1}{2} & 0 \\ 0 & \frac{1}{\sqrt{2}} & \frac{1}{\sqrt{2}} & 0 \end{pmatrix}. \quad (\text{B10})$$

Similarly, to find the action of the deformed unitary X_θ on two qubits we first let it act trivially on the state $|\tilde{3}\rangle$, as in (B6), and perform the change of basis (B8) obtaining $X_{2 \times 2} \rightarrow X_\theta$,

$$X_\theta = \begin{pmatrix} x_0(\theta) & \frac{1}{\sqrt{2}}x_2(\theta) & \frac{x_2(\theta)}{\sqrt{2}} & x_1(\theta) \\ \frac{x_1(\theta)}{\sqrt{2}} & \frac{1}{2}(1+x_0(\theta)) & \frac{1}{2}(-1+x_0(\theta)) & \frac{x_2(\theta)}{\sqrt{2}} \\ \frac{x_1(\theta)}{\sqrt{2}} & \frac{1}{2}(-1+x_0(\theta)) & \frac{1}{2}(1+x_0(\theta)) & \frac{x_2(\theta)}{\sqrt{2}} \\ x_2(\theta) & \frac{x_1(\theta)}{\sqrt{2}} & \frac{x_1(\theta)}{\sqrt{2}} & x_0(\theta) \end{pmatrix} \quad (\text{B11})$$

This operator gives the states $|1_\theta\rangle$ and $|2_\theta\rangle$ in the two qubit basis,

$$|1_\theta\rangle = x_0(\theta)|00\rangle + \frac{x_1(\theta)}{\sqrt{2}}(|01\rangle + |10\rangle) + x_2(\theta)|11\rangle \quad (\text{B12})$$

$$|2_\theta\rangle = x_0(2\theta)|00\rangle + \frac{x_1(2\theta)}{\sqrt{2}}(|01\rangle + |10\rangle) + x_2(2\theta)|11\rangle.$$

Appendix C: Parameterised Waveplates

The purpose of the experiment is to reproduce the probabilities $p_{a,b}(n) = |\langle n | \psi_{a,b} \rangle|^2$. Therefore, it is not necessary to reproduce the states $|\psi_{a,b}\rangle$, but only to match the modulus of the coefficients after projecting the state in the Z -basis, $q_{i,j} = |\langle i, j | \psi_{a,b} \rangle|^2$ with $i = 0, 1$ and $j = 0, 1$.

The experimental states $|\psi_{a,b}^{exp}\rangle$ produced by our setup depend on three parameters, $\vec{\alpha} = (\alpha_1, \alpha_2, \alpha_3)$, through the half-waveplates shown in Figure 5. We need to find the parameters $\vec{\alpha}_{opt}$ that best reproduce $q_{i,j}$. We simulate a noiseless version of the experimental setup obtaining the parameterized states $|\psi_{a,b}^{sim}(\vec{\alpha})\rangle$ and the overlaps $q_{i,j}^{sim}(\vec{\alpha})$. This allows us to get $\vec{\alpha}_{opt}$ as the solution to an optimization problem in which we aim to maximize the Hellinger fidelity F between $q_{i,j}$ and $q_{i,j}^{sim}(\vec{\alpha})$,

$$F(\vec{\alpha}) = \sum_{i,j} \sqrt{q_{i,j} q_{i,j}^{sim}(\vec{\alpha})}. \quad (\text{C1})$$

In order to reproduce the entanglement of the system, we also require that the entanglement entropies of the simulated states $S^{sim}(\vec{\alpha})$ reproduce the theoretical entropies S (see Figure 7c). Once again, this can be formulated as an optimization problem where the objective is to minimize $|S - S^{sim}(\vec{\alpha})|$. Taking into account this new term, we seek to minimize

$$C(\vec{\alpha}) = 1 - F(\vec{\alpha}) + |S - S^{sim}(\vec{\alpha})|, \quad (\text{C2})$$

so that $\vec{\alpha}_{opt} = \text{argmin}(C(\vec{\alpha}))$. The minimization is performed using the L - $BFGS$ - B algorithm [37] implemented in SciPy [38], reaching $C(\vec{\alpha}_{opt}) < 10^{-6}$ for all values of θ .

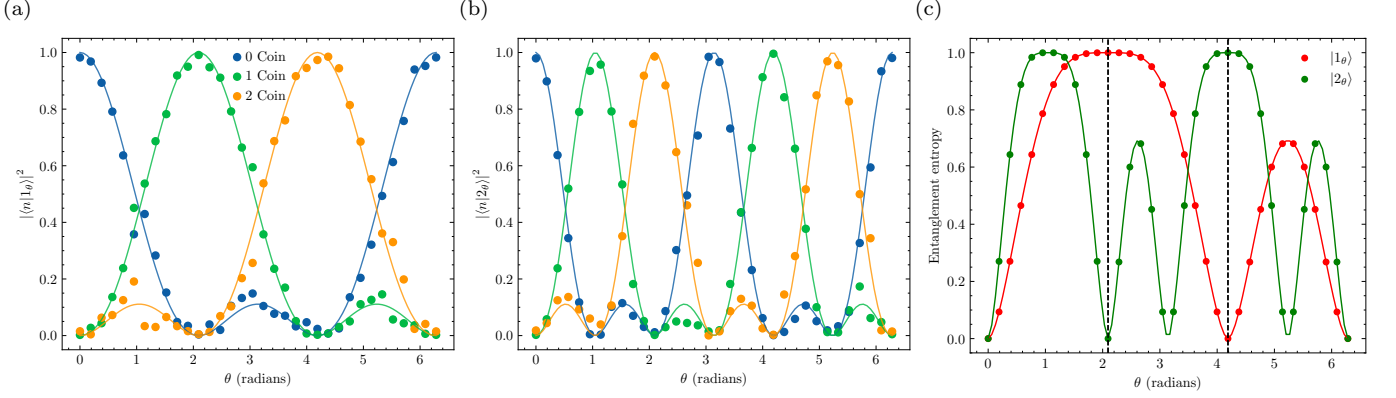


FIG. 7. Features of the states reproduced by our experimental setup. The theoretical (solid line) and experimental (dots) overlaps $|\langle n|1_\theta\rangle|^2$ and $|\langle n|2_\theta\rangle|^2$ with $n = 0$ (blue), 1 (green), 2 (orange) are shown in (a) and (b), respectively. The entanglement entropy of the states $|1_\theta\rangle$ and $|2_\theta\rangle$ is shown in (c). The entanglement entropy calculated by simulating the experimental setup without noise and using the optimal parameters for the half-wave plates after numerical optimization is indicated by dots.

Appendix D: Unitary decomposition

An arbitrary unitary $V \in U(4)$ can be implemented as a quantum circuit using local gates and three CNOTs [33]. Furthermore, it is possible to use only two CNOTs iff $\text{tr}[V(\sigma_y)^{\otimes 2}V^\dagger(\sigma_y)^{\otimes 2}]/\sqrt{\det(V)}$ is real [34]. This condition is satisfied for the deformed unitary (B11) when $\theta = 2\pi/3$ (classical case), $4\pi/3$. As indicated in the main text, $\theta = 4\pi/3$ reproduces the classical case under the interchange of states $|1\rangle$ and $|2\rangle$. This means that the θ -deformation introduces an additional CNOT gate.

The circuits

$$\begin{array}{c}
 \text{---} U(\beta_2, \pi/4, -\pi/3) \text{---} \bullet \text{---} R_X(-\pi/3) \text{---} \bullet \text{---} U(\beta_1, -2\pi/3, \pi/4) \\
 \text{---} U(\beta_1, 3\pi/4, 2\pi/3) \text{---} \oplus \text{---} R_Z(\pi/3) \text{---} \oplus \text{---} U(\beta_2, \pi/3, 3\pi/4) \\
 \text{(D1)}
 \end{array}$$

$$\begin{array}{c}
 \text{---} U(\beta_2, -\pi/4, -2\pi/3) \text{---} \bullet \text{---} R_X(-\pi/3) \text{---} \bullet \text{---} U(\beta_1, -\pi/3, -\pi/4) \\
 \text{---} U(\beta_1, -3\pi/4, \pi/3) \text{---} \oplus \text{---} R_Z(\pi/3) \text{---} \oplus \text{---} U(\beta_2, 2\pi/3, -3\pi/4) \\
 \text{(D2)}
 \end{array}$$

with $\beta_1 = \arccos(-1/3)/2$ and $\beta_2 = \pi - \beta_1$ implement (B11) for $\theta = 2\pi/3, 4\pi/3$, respectively. For the remaining values of θ , the circuits have the structure

$$\begin{array}{c}
 \text{---} U(\tilde{\alpha}_1) \text{---} \bullet \text{---} U(\tilde{\alpha}_3) \text{---} \bullet \text{---} U(\tilde{\alpha}_5) \text{---} \bullet \text{---} U(\tilde{\alpha}_7) \\
 \text{---} U(\tilde{\alpha}_2) \text{---} \oplus \text{---} U(\tilde{\alpha}_4) \text{---} \oplus \text{---} U(\tilde{\alpha}_6) \text{---} \oplus \text{---} U(\tilde{\alpha}_8) \\
 \text{(D3)}
 \end{array}$$

and the parameters $\tilde{\alpha}_j$ can be determined following the method proposed in [33].

Appendix E: General Quantum Morra Game

The game can be generalized to n players and m coins straightforwardly. Given a pool with $r = nm$ coins, each player can draw from 0 to m coins and guess the total number of coins, with the restriction that Bob cannot repeat Alice's guess. Similarly to the game with two players and one coin, we assign a state $|j\rangle$ to each possible total number of coins $j = 0, 1, \dots, r$. In the classical case, each player has an operator X_r that adds a coin when is applied to a state $|j\rangle$ with $j < r$, and $X_r^{r+1} = \mathbb{I}$. This operator is the $r + 1$ -dimensional generalization of the Pauli matrix σ_1 ,

$$X_r = \begin{pmatrix} 0 & 0 & 0 & \dots & 0 & 1 \\ 1 & 0 & 0 & \dots & 0 & 0 \\ 0 & 1 & 0 & \dots & 0 & 0 \\ 0 & 0 & 1 & \dots & 0 & 0 \\ \vdots & \vdots & \vdots & \ddots & \vdots & \vdots \\ 0 & 0 & 0 & \dots & 1 & 0 \end{pmatrix}, \quad \text{(E1)}$$

and it is related to the operator $Z_r = \text{diag}(1, \omega, \dots, \omega^r)$ with $\omega = e^{i2\pi/(r+1)}$ by means of the Fourier transform \mathcal{F} ,

$$X_r = \mathcal{F}^\dagger Z_r \mathcal{F}. \quad \text{(E2)}$$

Replacing Z_r by $\text{diag}(1, e^{i\theta}, \dots, e^{ri\theta})$ we get the deformed game and the modified $X_{r,\theta}$ operator which creates the states

$$|j_\theta\rangle = X_{r,\theta}^j |\tilde{0}\rangle = x_0(j\theta)|\tilde{0}\rangle + x_1(j\theta)|\tilde{1}\rangle + \dots + x_r(j\theta)|\tilde{r}\rangle \quad \text{(E3)}$$

with

$$x_a(\theta) = \frac{1}{r+1} \left(1 + \sum_{k=1}^r \omega^{(r+1-k)a} e^{ki\theta} \right). \quad \text{(E4)}$$

The generalized quantum Morra game can be implemented with $\lceil \log_2(r+1) \rceil$ qubits.

Appendix F: A Quantum Coin Deposit

It is well known that qubits belonging to a Bell pair are indistinguishable, this is a hallmark of entanglement. An intriguing consequence of our choice of encoding with a Bell pair results in the indistinguishability of the coins

played by either player. This may have application in anonymous, secure Quantum Deposit system, wherein the choices of the participants remain concealed. This system operates independently of classical communication channels, offering a sharp departure from traditional games like Morra, which rely on some level of communication. The Quantum Deposit model could lead to new security protocols that require untraceable transactions or enhanced privacy. While the exploration of these applications is beyond the scope of this paper, future researchers could delve into the development of quantum cryptographic methods that capitalize on this work.

-
- [1] John. Von Neumann and Oskar Morgenstern, *Theory of games and economic behavior*, 2nd rev. ed. (Princeton university press, 1947).
- [2] John F. Nash, “Equilibrium points in n -person games,” *Proceedings of the National Academy of Sciences* **36**, 48–49 (1950).
- [3] Stefano Ghirlanda and Giorgio Vallortigara, “The evolution of brain lateralization: a game-theoretical analysis of population structure,” *Proceedings of the Royal Society of London. Series B: Biological Sciences* **271**, 853–857 (2004).
- [4] Duncan Snidal, “The Game Theory of International Politics,” *World Politics* **38**, 25–57 (1985).
- [5] R. Duncan Luce and Howard Raiffa, *Games and decisions: introduction and critical survey* (Dover Publications, New York, 1989).
- [6] Yoav Shoham, “Computer science and game theory,” *Communications of the ACM* **51**, 74–79 (2008).
- [7] David A. Meyer, “Quantum Strategies,” *Physical Review Letters* **82**, 1052–1055 (1999).
- [8] Roman S. Ingarden, “Quantum information theory,” *Reports on Mathematical Physics* **10**, 43–72 (1976).
- [9] Charles H. Bennett and Gilles Brassard, “Quantum cryptography: Public key distribution and coin tossing,” *Theoretical Computer Science* **560**, 7–11 (2014).
- [10] Stephen Wiesner, “Conjugate coding,” *ACM SIGACT News* **15**, 78–88 (1983).
- [11] Omar Gustavo Zabaleta, Juan Pablo Barrangú, and Constancio M Arizmendi, “Quantum game application to spectrum scarcity problems,” *Physica A: Statistical Mechanics and its Applications* **466**, 455–461 (2017).
- [12] Jens Eisert, Martin Wilkens, and Maciej Lewenstein, “Quantum Games and Quantum Strategies,” *Physical Review Letters* **83**, 3077–3080 (1999).
- [13] Simon C Benjamin and Patrick M Hayden, “Multiplayer quantum games,” *Physical Review A* **64**, 030301(R) (2001).
- [14] Amit Anand, Bikash K Behera, and Prasanta K Panigrahi, “Solving diner’s dilemma game, circuit implementation and verification on the ibm quantum simulator,” *Quantum Information Processing* **19**, 1–14 (2020).
- [15] Neal Solmeyer, Norbert M Linke, Caroline Figgatt, Kevin A Landsman, Radhakrishnan Balu, George Siopsis, and Christopher Monroe, “Demonstration of a bayesian quantum game on an ion-trap quantum computer,” *Quantum Science and Technology* **3**, 045002 (2018).
- [16] Richard E George, Lucio M Robledo, Owen JE Maroney, Machiel S Blok, Hannes Bernien, Matthew L Markham, Daniel J Twitchen, John JL Morton, G Andrew D Briggs, and Ronald Hanson, “Opening up three quantum boxes causes classically undetectable wavefunction collapse,” *Proceedings of the National Academy of Sciences* **110**, 3777–3781 (2013).
- [17] Robert Prevedel, André Stefanov, Philip Walther, and Anton Zeilinger, “Experimental realization of a quantum game on a one-way quantum computer,” *New Journal of Physics* **9**, 205 (2007).
- [18] ARC Pinheiro, CER Souza, DP Caetano, JAO Huguenin, AGM Schmidt, and AZ Khoury, “Vector vortex implementation of a quantum game,” *JOSA B* **30**, 3210–3214 (2013).
- [19] Christian Schmid, Adrian P Flitney, Witlef Wieczorek, Nikolai Kiesel, Harald Weinfurter, and Lloyd CL Hollenberg, “Experimental implementation of a four-player quantum game,” *New Journal of Physics* **12**, 063031 (2010).
- [20] W F Balthazar, M H M Passos, A G M Schmidt, D P Caetano, and J A O Huguenin, “Experimental realization of the quantum duel game using linear optical circuits,” *Journal of Physics B: Atomic, Molecular and Optical Physics* **48**, 165505 (2015).
- [21] Indrakshi Dey, Nicola Marchetti, Marcello Caleffi, and Angela Sara Cacciapuoti, “Quantum game theory meets quantum networks,” arXiv preprint arXiv:2306.08928 (2023).
- [22] Gaius Suetonius, *The lives of the twelve Caesars* (BoD—Books on Demand, 2019).
- [23] Peter Morris, *Introduction to game theory* (Springer Science & Business Media, 2012).
- [24] Luis Pastor-Abia, José M. Pérez-Jordá, Emilio San-Fabián, Enrique Louis, and Fernando Vega-Redondo, “Strategic behavior and information transmission in a stylized (so-called *Chinos*) guessing game,” *Advances in Complex Systems* **04**, 177–190 (2001).
- [25] Luis Pastor-Abia, Emilio San-Fabián, Enrique Louis, and Fernando Vega-Redondo, “Learning to play in a stylized (*Chinos*) game: some preliminary results,” in *AIP Conference Proceedings*, Vol. 661 (American Institute of Physics, 2003) pp. 167–173.
- [26] F Guinea and M A Martín-Delgado, “Quantum *Chinos* game: winning strategies through quantum fluctuations,”

- Journal of Physics A: Mathematical and General* **36**, L197–L204 (2003).
- [27] Daniel Centeno and Germán Sierra, “General quantum chinos games,” *Journal of Physics Communications* **6**, 075009 (2022).
- [28] Irving L Glicksberg, “A further generalization of the kakutani fixed theorem, with application to nash equilibrium points,” *Proceedings of the American Mathematical Society* **3**, 170–174 (1952).
- [29] Cristina Bicchieri, “Rationality and game theory,” in *The Oxford Handbook of Rationality*, edited by Alfred R. Mele and Piers Rawling (Oxford University Press, 2004) 1st ed., Chap. 10, pp. 182–205.
- [30] Gholamreza Askari, Madjid Eshaghi Gordji, and Choonkil Park, “The behavioral model and game theory,” *Palgrave Communications* **5** (2019).
- [31] Sundus Naseer, Qurratul-Ain Minhas, Khalid Saleem, Ghazanfar Farooq Siddiqui, Naeem Bhatti, and Hasan Mahmood, “A game theoretic power control and spectrum sharing approach using cost dominance in cognitive radio networks,” *PeerJ Computer Science* **7**, e617 (2021).
- [32] Vilfredo Pareto, “The maximum of utility given by free competition,” *Giornale degli Economisti e Annali di Economia* **67 (Anno 121)**, 387–403 (2008).
- [33] G. Vidal and C. M. Dawson, “Universal quantum circuit for two-qubit transformations with three controlled-NOT gates,” *Physical Review A* **69**, 010301(R) (2004).
- [34] Vivek V. Shende, Stephen S. Bullock, and Igor L. Markov, “Recognizing small-circuit structure in two-qubit operators,” *Physical Review A* **70**, 012310 (2004).
- [35] Alessandro Fedrizzi, Thomas Herbst, Andreas Poppe, Thomas Jennewein, and Anton Zeilinger, “A wavelength-tunable fiber-coupled source of narrowband entangled photons,” *Optics Express* **15**, 15377–15386 (2007).
- [36] Alexander Pickston, Joseph Ho, Andrés Ulibarrena, Federico Grasselli, Massimiliano Proietti, Christopher L Morrison, Peter Barrow, Francesco Graffitti, and Alessandro Fedrizzi, “Conference key agreement in a quantum network,” *npj Quantum Information* **9**, 82 (2023).
- [37] Richard H. Byrd, Peihuang Lu, Jorge Nocedal, and Ciyou Zhu, “A Limited Memory Algorithm for Bound Constrained Optimization,” *SIAM Journal on Scientific Computing* **16**, 1190–1208 (1995).
- [38] Pauli Virtanen, Ralf Gommers, Travis E. Oliphant, Matt Haberland, Tyler Reddy, David Cournapeau, Evgeni Burovski, Pearu Peterson, Warren Weckesser, Jonathan Bright, Stéfan J. van der Walt, Matthew Brett, Joshua Wilson, K. Jarrod Millman, Nikolay Mayorov, Andrew R. J. Nelson, Eric Jones, Robert Kern, Eric Larson, C J Carey, İlhan Polat, Yu Feng, Eric W. Moore, Jake VanderPlas, Denis Laxalde, Josef Perktold, Robert Cimrman, Ian Henriksen, E. A. Quintero, Charles R. Harris, Anne M. Archibald, Antônio H. Ribeiro, Fabian Pedregosa, Paul van Mulbregt, and SciPy 1.0 Contributors, “SciPy 1.0: Fundamental Algorithms for Scientific Computing in Python,” *Nature Methods* **17**, 261–272 (2020).
- [39] Francesco Graffitti, Peter Barrow, Massimiliano Proietti, Dmytro Kundys, and Alessandro Fedrizzi, “Independent high-purity photons created in domain-engineered crystals,” *Optica* **5**, 514–517 (2018).
- [40] Alexander Pickston, Francesco Graffitti, Peter Barrow, Christopher L. Morrison, Joseph Ho, Agata M. Brańczyk, and Alessandro Fedrizzi, “Optimised domain-engineered crystals for pure telecom photon sources,” *Opt. Express* **29**, 6991–7002 (2021).
- [41] Erwin Schrödinger, “Discussion of probability relations between separated systems,” in *Mathematical Proceedings of the Cambridge Philosophical Society*, Vol. 31 (Cambridge University Press, 1935) pp. 555–563.
- [42] H. M. Wiseman, S. J. Jones, and A. C. Doherty, “Steering, entanglement, nonlocality, and the einstein-podolsky-rosen paradox,” *Phys. Rev. Lett.* **98**, 140402 (2007).
- [43] Massimiliano Proietti, Joseph Ho, Federico Grasselli, Peter Barrow, Mehul Malik, and Alessandro Fedrizzi, “Experimental quantum conference key agreement,” *Science Advances* **7**, eabe0395 (2021).
- [44] Faisal Shah Khan, Neal Solmeyer, Radhakrishnan Balu, and Travis S Humble, “Quantum games: a review of the history, current state, and interpretation,” *Quantum Information Processing* **17**, 1–42 (2018).